J Neuropathol Exp Neurol
Vol. 69, No. 1
January 2010
pp. 98–108

ORIGINAL ARTICLE

Amyloid Deposition and Influx Transporter Expression at the Blood-Brain Barrier Increase in Normal Aging

Gerald D. Silverberg, MD, Miles C. Miller, ScB, Arthur A. Messier, PhD, Samir Majmudar, BA, Jason T. Machan, PhD, John E. Donahue, MD, Edward G. Stopa, MD, and Conrad E. Johanson, PhD

Abstract

Aging is the most important single risk factor for developing Alzheimer disease. We measured amyloid-β peptide (Aβ) levels in rat cerebral cortex and hippocampus during normal aging of Brown-Norway/Fischer rats. Amyloid-β accumulation was associated with expression of the Aβ influx transporter, the receptor for advanced glycation end-products (RAGEs) at the blood-brain barrier. Rats at selected ages from 3 to 36 months were analyzed by 1) immunohistochemistry for amyloid deposition and quantitative microvessel surface area RAGE expression, 2) ELISA for cortical Aβ40 and Aβ42 concentrations, and 3) Western blotting of microvessel proteins for RAGE expression. Immunohistochemistry showed increasing accumulation of brain Aβ with aging. By ELISA analysis, both Aβ40 and Aβ42 concentrations in cortical homogenates rose sharply from 9 to 12 months. The Aβ42 continued to rise up to age 30 months, whereas Aβ40 stabilized after 12 months. The expression of RAGE initially decreased between 3 and 12 months but then increased between 12 and 34 months by immunohistochemistry. On immunoblotting, RAGE decreased up to 9 months and then progressively increased up to 36 months. These data indicate an association between amyloid and microvessel RAGE during aging. An increase in capillary RAGE expression seems to play a role in the later Aβ accumulation but not in the initial increase.

Key Words: Aging, Amyloid, Blood-brain barrier, RAGE, Transport.

INTRODUCTION

Advancing age is considered to be the single most important risk factor for the development of Alzheimer disease (AD) (1–3). There seems to be a continuum in amyloid-β peptide (Aβ) accumulation from normal aging to AD, although the molecular basis for this transition is not yet clear. The increasing amyloid burden in AD is thought to be an important component of AD pathogenesis (3–6). It has been suggested by many authors that the failure to clear Aβ from the extracellular fluid space of the brain plays an important role in the genesis and progression of AD (7–10).

Amyloid-β peptide efflux transport across the blood-brain barrier (BBB) is a critical pathway for Aβ clearance from the brain, but Aβ transport seems to be bidirectional and may be concentration dependent in healthy young adults (11, 12). Amyloid-β peptide BBB efflux transport is via the low-density lipoprotein receptor–related protein 1 (LRP-1) and P-glycoprotein (P-gp) (13, 14). Influx transport is mediated by the endothelial cell receptor for advanced glycation end-products (RAGEs) (15). Brain Aβ was initially thought to derive solely from neurons and glia within the CNS (16, 17). It is now believed that influx transport of plasma Aβ across the capillary endothelium that is mediated by RAGE expression may be an important source (11, 18–20).

The RAGE is expressed in the brain on some neuronal membranes and on the luminal surface of capillary endothelial cells. It is a signal transduction receptor member of the immunoglobulin cell surface molecule superfamily with a number of isoforms that may be functionally important (21–23). The RAGE interacts with AGEs, the products of nonenzymatic glycosylation and oxidation of proteins and lipids. The AGEs accumulate in normal aging and in many diseases and pro-oxidant states. The AGEs are formed primarily by the reaction of sugars with the amino groups of lysine and arginine (21, 24, 25). The binding of AGEs to RAGE is thought to be damaging to endothelium in aging and in disease states (26).

The RAGE also functions as a receptor/transporter for Aβ and β-sheet fibrils (15, 27). The RAGE expression has been shown to increase in AD, among other chronic diseases (e.g. diabetes mellitus, atherosclerosis, and cardiovascular disease), chronic inflammatory diseases, renal failure, and cancer (19, 20, 28, 29). Upregulation of RAGE expression is mediated by several ligands, including AGEs and Aβ, and by cytokines such as interleukin 1 and tumor necrosis factor by activating nuclear factor-κB (30–33).

We have previously shown in brain bank specimens that there are significant alterations in the expression of amyloid transport receptor proteins at the BBB in AD compared with age-matched human controls (19, 20); this also seems to be the

From the Department of Clinical Neuroscience, Warren Alpert Medical School, Brown University and Aldrich Neurosurgery Research Laboratories, Rhode Island Hospital, (GDS, MCM, AAM, SM, CEJ); Biostatistics, Rhode Island Hospital-Lifespan (JTM); and Division of Neuropathology, Department of Pathology, Warren Alpert Medical School, Brown University and Aldrich Neuropathology Laboratories, Rhode Island Hospital (JED, EGS), Providence, Rhode Island.

Send correspondence and reprint requests to: Gerald D. Silverberg, MD, 710 Frenchman's Rd, Stanford, CA 94305; E-mail geralds@stanford.edu

This study was supported by Grant No. 1RO1 AG027910-01 from the National Institutes of Health, by the Saunders Family Fund, and by the Rae and Jerry Richter AD Research Fund.

Supplemental digital content is available for this article. Direct URL citations appear in the printed text and are provided in the HTML and PDF versions of this article on the journal's Web site (www.jneuropath.com).

case in some animal models of AD (34). Expression of the capillary amyloid efflux transporter LRP-1 is decreased, whereas the expression of the amyloid influx transporter RAGE is increased (19). Furthermore, there is a progressive increase in microvessel RAGE expression from controls through early-stage AD to late-stage AD (20).

Here, we investigated brain Aβ accumulation and RAGE expression on brain capillary endothelium in the aging rat to determine when Aβ begins to accumulate and whether there is an associated increase in BBB RAGE expression, similar to that observed in AD. We report the progressive increase in microvessel RAGE expression after 12 months of age and its temporal relationship to the measured progressive brain amyloid burden beginning between 6 and 9 months in the aging Brown-Norway/Fischer (BN/F) rat.

MATERIALS AND METHODS

Animals and In Situ Perfusion

Male BN/F rats (n = 188) at ages 3 through 36 months were examined. The BN/F rats were chosen because they are long-lived and develop less neoplasia with aging than more inbred strains. Moreover, unlike larger species that develop Aβ plaques, the life span and availability of the BN/F rats made them an attractive model for studying aging rather than the development of AD. We were able to obtain this strain at most ages up to 36 months from the National Institute of Aging colony. The rats were housed in the Central Animal Facility at Rhode Island Hospital and were provided food and water ad libitum. The Institutional Animal Care and Use Committee at Rhode Island Hospital approved all experiments. Rats were euthanized with intraperitoneal pentobarbital (125 mg/kg) and perfused with PBS via left ventricular cannulation. Twenty-two rats used for immunohistochemistry (IHC) were then perfused with 4% paraformaldehyde; their brains were quickly removed and stored at −80°C until used. For ELISA measurements, the brains of 30 rats were also quickly removed and stored at −80°C immediately after the PBS perfusion. The remaining rats were used for microvessel isolations (MVIs).

Amyloid Immunohistochemistry

Ten-micrometer-thick, 4% paraformaldehyde–fixed, paraffin-embedded tissue sections were incubated in an oven at 60°C for 1 hour and then deparaffinized and rehydrated. After a 20-minute pretreatment with hot (85°C) 10-mmol/L citrate buffer (pH 6.0), sections were quenched with 3% H_2O_2 and 50% methanol, diluted in distilled water, for 10 minutes. Nonspecific binding sites were blocked by incubation with 5% normal goat serum (Vector Laboratories, Burlingame, CA) for 2 hours at room temperature (RT) before incubation with the primary antibody: either rabbit polyclonal Aβ40, diluted 1:50 (Linaris, Catalog No. PAK6021, Wertheim-Bettingen, Germany), or Aβ42, diluted 1:200 (Linaris, Catalog No. PAK6023), overnight at 4°C. The sections were then washed with Tris-buffered saline (TBS) with Tween-20 (TBST) and subjected to a modified ABC technique using the Vectastain Elite ABC Rabbit Peroxidase system (Vector) with 3,3-diaminobenzidine (Vector) as the chromogen. Slides were coverslipped and sealed using Cytoseal, a xylene-based mounting medium (Stevens Scientific, Riverdale, NJ). Primary antibody omission controls were run alongside the other samples to check for nonspecific binding caused by the secondary antibody, along with positive control tissue (human hippocampus with Braak and Braak Stage VI AD pathology).

RAGE Immunohistochemistry

Specimens were snap frozen in liquid N_2, embedded in OCT compound (Sakura Finetek USA, Inc, Torrance, CA), and cryosectioned at a thickness of 25 μm. After a quick rinse in TBST, sections were quenched in 10% H_2O_2 for 10 minutes to block endogenous peroxidase activity, followed by a 24-hour blocking period with 5% normal goat serum (Vector) at 4°C. After an overnight incubation at 4°C with a rabbit polyclonal RAGE antibody (1:400; Affinity Bioreagents, Catalog No. PA1-075, Golden, CO), the sections were washed with TBST before application of the secondary antibody. A goat anti-rabbit IgG diluted 1:500 (Vector) was applied for 30 minutes at RT. The ABC detection system (Vector) was used, and the tissue sections were stained using 3,3-diaminobenzidine as the chromogen. Sections were mounted, and slides were coverslipped and sealed as previously described. Primary antibody omission negative controls and positive control (rat lung) were run alongside the other samples.

Image Analysis

Grayscale images were obtained using an Olympus BH2-RFCA microscope (Olympus America, Inc, Mellville, NY) using a 40× objective. Images were acquired with a CoolSNAP cf camera (Roper Scientific, Tucson, AZ). Random fields (n = 8) were analyzed per specimen (n = 3 per age group; 24 fields per group) to confirm the presence of RAGE in relation to capillary endothelia. Cross sections of cerebral microvessels 10 to 20 μm in diameter were selected in each of the 8 random field images acquired per specimen. Image processing and analysis were performed using NIH Image shareware (National Institutes of Health, Springfield, VA) along with previously reported methods (35, 36). For surface area calculations, all images were analyzed by the same user at a single sitting to reduce errors associated with this mode of analysis. Using the average of the 8 collected surface areas of capillary endothelial immunoreaction product per animal, statistics were performed as described later.

Aβ ELISA

Concentrations of Aβ40 and Aβ42 in cortical rat brain samples were measured using a sandwich ELISA method (n = 5 for each age group). High-sensitivity ELISA kits (Wako Chemicals, Catalog Nos. 294-64701 and 292-64501, Richmond, VA) were chosen to reduce background and to improve detection of Aβ40 (sensitivity, 0.049 pmol/L) and Aβ42 (sensitivity, 0.024 pmol/L). Both kits use a 2–binding site sandwich ELISA system designed to specifically detect Aβ40 and Aβ42. A monoclonal antibody directed against Aβ11-28 (BNT77) was used as the capture antibody. It detects full-length Aβ and Aβ with a truncated or modified

N-terminus. For specific detection of Aβ40, the monoclonal antibody BA27 directed against the C-terminal portion of Aβ40 was used, and for Aβ42, BC05 directed against the C-terminal portion of Aβ42 was used. Although highly unlikely (given the high specificity of the kits), cross-reactivity of the C-terminal antibodies with other proteins cannot be excluded (37, 38) (Appendix).

Samples of brain tissue were snap frozen in liquid N_2 and then ground into a powder on a bed of dry ice. A 100-mg aliquot of the powder for each sample was transferred to a 1.5-mL conical microtube and extracted by sonication with 1 mL of a 0.2% diethylamine/50 mmol/L NaCl solution. Samples were centrifuged at 16,000 rpm for 2 hours at 4°C, followed by removal of the supernatant (saved as the 0.2% diethylamine extract). Formic acid (70%) was then added to each tube, and the pellet was resonicated. Samples were again centrifuged at 16,000 rpm for 2 hours at 4°C, followed by removal of the supernatant (saved as the formic acid extract). The 0.2% diethylamine–extracted supernatants were diluted 10-fold with 0.5 mol/L Tris-HCl (pH 6.8) for neutralization and vortexed, followed by dilution in 10 volumes of PBS supplemented with 1× protease inhibitor cocktail (P-2714; Sigma-Aldrich, St Louis, MO). For the formic acid–extracted supernatants, samples were neutralized by a 20-fold dilution with 1 mol/L Tris Base. The Aβ40 and Aβ42 concentrations were measured using ELISA kits (Wako Chemicals) according to the manufacturer's instructions. Samples and standards were diluted with the kit standard diluent and added in duplicate to antibody-coated wells of a 96-well microtiter plate. The plates were incubated overnight at 4°C. After washing, samples were incubated for 2 hours (Aβ40) or 1 hour (Aβ42) at 4°C in 100 μL of horseradish peroxidase–conjugated antibody solution. The color was evolved by adding 100 μL of a 3,3′,5,5′-tetramethylbenzidine–containing solution to the wells, and the reactions were terminated 30 minutes later using the kit stop solution. The plate was read on a Multiskan Plus spectrophotometer at 450 nm, and data were analyzed using DeltaSoft3 software. The total protein content of each sample was determined using a BCA Protein Assay kit (Pierce, Rockford, IL), with absorbance read at 562 nm. Total Aβ concentrations were expressed as picograms per milligram total protein.

Microvessel Isolation and Western Blots

For MVI, the meninges were removed and the brains were placed in ice-cold PBS. The cerebellum, most subcortical structures, and choroid plexus tissues were also removed, leaving the cortex and hippocampus. To obtain sufficient microvessels for analysis, 4 rat brains were used for a single *n* at each age point, that is, *n* of 4 = 16 brains. A total of 136 rats were necessary for this analysis. Microvessels were isolated by homogenizing cortex and hippocampus in MVI buffer (103 mmol/L NaCl, 15 mmol/L HEPES, 10 mmol/L glucose, 4.7 mmol/L KCl, 2.5 mmol/L $CaCl_2$, 2.5 mmol/L $NaHCO_3$, 1.2 mmol/L K_3PO_4, 1.2 mmol/L $MgSO_4$, 1 mmol/L sodium pyruvate, 1% wt/vol dextran), then adding 26% dextran solution to achieve an approximately 13% dextran/MVI buffer (all chemicals from Sigma). The microvessels were then separated using a basic mechanical separation technique, that is, repeated centrifugation at 4°C, resuspension of the pellets in dextran/MVI buffer, and in most cases, by passage of the MVI through a 100-μm filter and microvessel capture on a 20-μm filter or by adherence to a glass bead column, as previously described (39). The MVI pellets were treated with protein lysis buffer (Complete Protease Inhibitor Product No. 13191000, Roche Diagnostics Mannheim, Germany) and frozen at −80°C in preparation for protein extraction.

The total protein content of each sample was determined using a BCA Protein Assay kit (Pierce), with absorbance read at 562 nm. The MVIs were tested for contamination by other CNS cell types by light microscopy, after staining with hematoxylin and eosin, and by Western blotting for neuron-specific enolase (NSE), the glial cell marker S100b, and glial fibrillary acidic protein (GFAP). Although it is not possible by the MVI separation method to achieve 100% microvessel purity, we could achieve greater than 95% clean vessels. Only MVIs with little (optical density [OD] <3% of the cortical homogenate OD values) or no neuronal or glial cell membrane contamination were used in the Western blot assessment of RAGE expression.

Approximately 3 mg of microvessels or rat cortex (positive control) were homogenized in protein lysis buffer (Complete Protease Inhibitor Product No. 13191000, Roche). One milliliter of each homogenate was centrifuged at 10,000 × *g* for 15 minutes. Protein concentrations were determined using bicinchoninic protein assay reagent (Pierce). Fifty micrograms of each sample was added to NUPAGE sample buffer (Invitrogen, Grand Island, NY). Samples were heated to 95°C for 2 minutes and spun briefly at 1,000 × *g*. Samples were run on 4% to 12% NUPAGE Novex Bis-Tris gels in running buffer (Invitrogen) at 200v for 35 minutes. Protein was transferred wet in NUPAGE transfer buffer (Invitrogen). Membranes were stained with Ponceau S, and then blocking serum (5% nonfat milk; Sigma) was applied. The following primary antibodies and dilutions were used: RAGE, 1:10,000 (polyclonal rabbit, no. PA1-075; Affinity Bioreagents); S-100b 1:10,000 (mouse monoclonal, no. ab4066; Abcam, Cambridge, MA); β-actin, 1:10,000 (mouse monoclonal, no. A 5441; Sigma); GFAP, 1:1000 (mouse monoclonal, no. ab10062; Abcam); and NSE, 1:10,000 (polyclonal rabbit, no. ab16873; Abcam). Secondary antibody was used at a concentration of 1:50,000. Western Blotting Detection Reagent (Supersignal West Pico Enhanced ECL, Pierce) was added, and blots were developed. Controls established the specificity of the antibodies used in the Western blotting analyses. Negative controls were used to ensure that no protein species could be detected on immunoblots when proteins were incubated with preimmune serum or by incubating without the primary antibody.

Statistical Methods

All statistical analyses were carried out using SAS version 9.2 (SAS Institute, Cary, NC). Increases in Aβ40 and Aβ42 concentrations over time were initially compared with their respective concentrations at the 3-month time point by 1-way analysis of variance, with multiple comparisons adjusted by the Bonferroni method. Means, SEs, and p values (analysis of variance) are reported for each age group

primarily for context. Piecewise regressions using PROC MIXED were used to test for changes in amyloid concentration and RAGE expression and to compare the changes in these metrics over time. The assumption of homogeneity of regression was verified by first running the model with covariance parameters for each age group and checking the null model likelihood ratio test for the covariance parameters. The Aβ40 and Aβ42 had variances that systematically increased with their mean in their natural scale, but which were corrected using a square-root transformation. The transformed values were also better fit by the accelerating accumulation of the model for the first several ages, although it still overestimated values at 9 months for both amyloid peptides. A more complex curve (logistic) would be more appropriate for the shape but could not be used because there were insufficient ages for which to fit relative to the number of parameters. All models satisfied the homogeneity of regression assumption; therefore, the covariance parameters were removed in the models presented, reducing them to piecewise regressions with 2 phases. The slope for the first phase for surface area RAGE was between 3 and 12 months and represented a simple comparison of means, which was expressed as such by setting the coefficient of the contrast to 9.

Three effects were tested in each model: 1) the phase 1 slope was compared with 0 (early accumulation); 2) the phase 2 slope was compared with 0 (late accumulation); and 3) the phase 1 slope was compared with the phase 2 slope (change in rate of accumulation). The first and third comparisons were part of the omnibus model (age, offset age phase); the second comparison was not and was carried out post hoc. Despite being a single planned follow-up comparison, this p value was adjusted for α inflation by a factor of 2 using the Bonferroni adjustment to be conservative.

RESULTS

Amyloid Accumulation

As indicated by both IHC and by ELISA, amyloid accumulated during the course of aging in the BN/F rat model (Fig. 1). There was only scant staining of Aβ42 by IHC at 3, 6, and 9 months (not shown). At 12 months, there was increased Aβ42 staining in cortical neurons in and around cortical and hippocampal blood vessels, in the lateral ventricle choroid plexus epithelium, and in ependymal cells (Fig. 1A). This staining was much more evident at 30 months and was diffusely apparent in the cortical parenchyma and in neurons and meninges; it was even more evident in perivascular spaces (Fig. 1B). A remarkable increase in granular neuronal Aβ42 staining in the cortex and hippocampus was prominent in the 30-month animals compared with the earlier age groups; these granular Aβ42 accumulations likely represent some degree of self-aggregation. Unlike Aβ42, there was moderate Aβ40 staining in cortical neurons and around blood vessels at 3 months and progressive increase in staining through 30 months. In addition, there was widespread granular neuronal Aβ40 staining throughout the hippocampus at 30 months.

The ELISA measurements for Aβ40 and Aβ42 confirmed the accumulation seen on IHC. Figure 1C compares all older age groups to the 3-month age group for both peptides. The ELISA measurements also demonstrated a difference in the accumulation profiles of the 2 peptides. These apparent differences were measured by slope analysis (Fig. 2). At 3 months, the Aβ40 concentration was 1.64 ± 0.49 pg/mg total protein (mean ± SEM). The concentration rose to 6.62 ± 1.22 pg/mg by 12 months (slope, 0.1484 ± 0.0260 root [pg/mg]/month, $p < 0.00001$). The Aβ40 concentration then leveled to 6.64 ± 0.47 at 20 months and 5.12 ± 0.7 pg/mg at 30 months (change in slope, −0.1549 ± 0.0352 root [pg/mg]/month, $p = 0.00002$; slope, −0.0065 ± 0.0133 root [pg/mg]/month, $p = 1.0$; Fig. 2A). The Aβ42 concentration increased in a similar fashion, measuring 0.07 ± 0.03 pg/mg at 3 months and rising to 9.45 ± 1.29 at 12 months (slope, 0.3044 ± 0.0243 root [pg/mg]/month, $p < 0.00001$). In contrast to Aβ40, which no longer accumulated significantly after 12 months, the concentration of Aβ42 continued to increase (slope, 0.0495 ± 0.0124 root [pg/mg]/month, $p = 0.001$; Fig. 2B) but at a slower rate (change in slope, −0.2548 ± 0.0328 root [pg/mg]/month, $p < 0.00001$). The Aβ42 concentration rose to 11.23 ± 0.8 at 20 months and 13.37 ± 0.83 pg/mg at 30 months. These changes represent an approximately 3- to 4-fold increase in Aβ40 concentration but an almost 200-fold increase in Aβ42 concentration during the lifetime of the rat.

Microvessel Isolations

Figure 3A shows an example of an MVI by light microscopy. The microvessels are intact with no evidence of other CNS cells or debris. Immunoblots for NSE, a generally accepted marker for neuronal cell membranes, showed minimal evidence of NSE in the MVI compared with control cortical homogenates. Immunoblots for S100b, which is expressed only on glial soma also showed little expression (Fig. 3B). A representative immunoblot age range for microvessel RAGE expression is shown in Figure 3C. The RAGE was expressed only on capillary endothelial cells and on neurons in the rat brain by IHC (Fig. 4). We found no evidence of RAGE immunostaining on either astrocytes or oligodendrocytes.

All MVI immunoblots were run alongside a cortex sample. After RAGE content was measured, the blot was stripped and tested for NSE and S100b contamination using the cortex sample as the positive control. The fraction of NSE and S100b contamination of the MVI samples was calculated with cortex as 1.00. The fraction of NSE contamination was 0.018 ± 0.002 (mean ± SEM) and that of S100b was 0.022 ± 0.003 for the 31 samples used. There were 3 samples in which the NSE contamination was 0.105 ± 0.005 and 0.113 ± 0.008 for S100b. These samples were excluded from the Western blot RAGE analysis. Because we saw no evidence on Western blot for significant amounts of NSE or for S100b, we are confident that the MVIs used for Western blot analysis of RAGE expression were relatively free of other RAGE-expressing cell populations (<3% compared with cortex).

Expression of the Aβ Influx Transporter RAGE

Immunohistochemistry and Western blotting quantified microvessel expression of RAGE over time in the cortex and

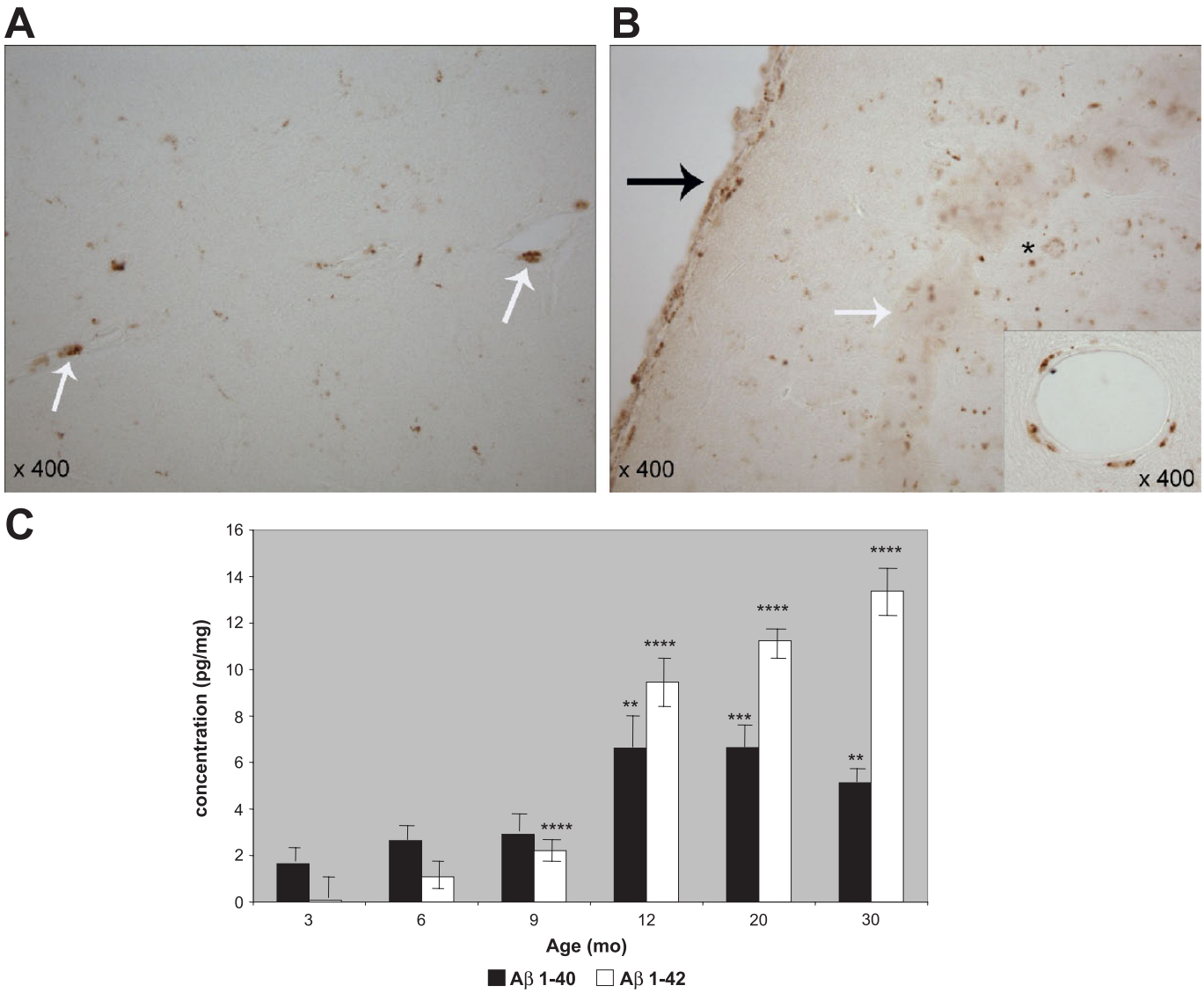

FIGURE 1. Amyloid accumulation analyzed as a function of aging in the Brown-Norway/Fischer (BN/F) rat. **(A)** Amyloid-β42 (Aβ42) immunohistochemistry at 12 months showing cortical amyloid accumulation in perivascular spaces (arrows). **(B)** Amyloid-β42 staining at 30 months showing diffuse cortical staining in the parenchyma (white arrow), around cerebral microvessels (inset), along the meninges (black arrow), and in neurons (asterisk). **(C)** Bar graph of Aβ40 and Aβ42 ELISA concentrations in brain homogenates in normal aging in the BN/F rat. Mean ± SEM; n = 5 rats per age group. p values (analysis of variance) compare the age group cited to the 3-month-old rat. ** $p < 0.01$, *** $p < 0.001$, **** $p < 0.0001$.

hippocampus. Immunohistochemistry expression of RAGE on microvessels and on neurons at 3 and 30 months is shown in Figure 4. At 3 months, neuronal RAGE immunoreactivity was widespread and robust, but it became less evident in the BN/F rat as a function of age. In contrast, RAGE expression in microvessels decreased between 3 and 12 months and then increased thereafter. The RAGE, as measured by microvessel surface area staining on multiple immunostained sections, was expressed as normalized surface area in square micrometers. The normalized surface area of microvessel staining for RAGE at 3 months was 12.2 ± 0.71 μm^2 (mean ± SEM); at 12 months, RAGE surface area staining trended lower, but not significantly so, to 10.7 ± 0.32 μm^2 (change, −2.3464 ± 1.9782 μm^2, $p = 0.2585$). After 12 months, RAGE expression increased (change in slope, 1.0894 ± 0.2787 μm^2/month, $p < 0.0001$), rising more or less linearly through 34 months (slope, 0.8287 ± 0.0875 μm^2/month, $p < 0.00001$). At 23 months, it was 16.95 ± 2.69 μm^2; at 30 months, it was 25.67 ± 1.03 μm^2; and at 34 months, it had risen to 28.36 ± 1.03 μm^2 (Fig. 5A).

Analysis of Western blotting for microvessel RAGE expression showed remarkable similarity to RAGE expression as measured by IHC surface areas with improved resolution. After observing the decrease in RAGE expression between 3 and 12 months by IHC, we added a 6- and 9-month age group to the immunoblots. Relative RAGE expression was reported

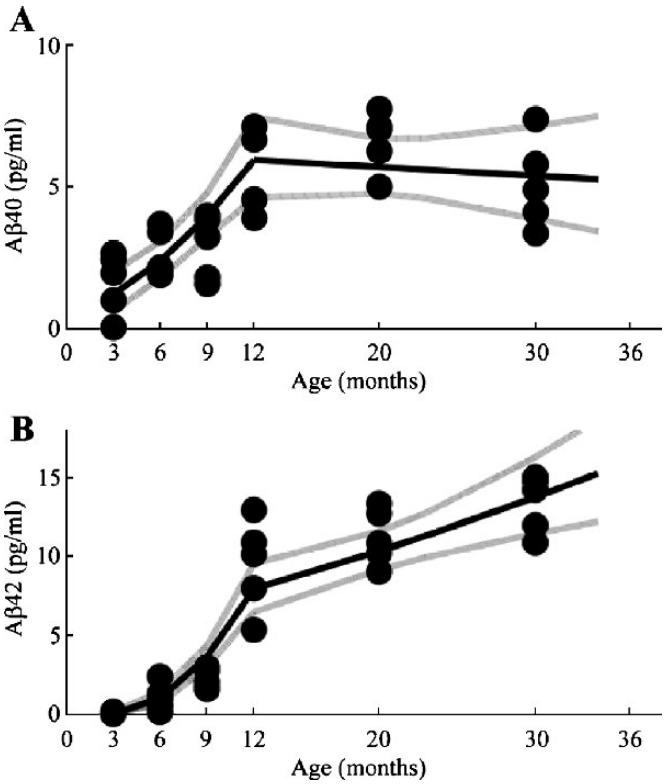

FIGURE 2. Piecewise regression of root amyloid-β40 (Aβ40) and root Aβ42 accumulation as a function of age. **(A)** Amyloid-β40 concentration rose from 3 to 12 months ($p < 0.0001$). The rate of increase was reduced thereafter ($p = 0.00002$) and did not increase significantly after 12 months ($p = 1.0$). **(B)** Amyloid-β42 also rose between 3 and 12 months ($p < 0.0001$) and then continued to rise to 30 months ($p = 0.001$) but at a slower rate ($p < 0.00001$). The most rapid increase in both peptides appeared between 9 and 12 months. Gray lines indicate the 95% confidence band.

as the blot OD, estimated by pixel density. Optical density mean values decreased monotonically from 3- to 9-month-old rats, suggestive of a negative trend during the first 9 months, but the trend did not quite reach significance (slope, -0.9535 ± 0.5729 OD units/month, $p = 0.1072$). After 9 months, RAGE OD values progressively increased through 36 months, although the expression at 12 months was still slightly lower than that at 3 months (slope, 0.6528 ± 0.1273 OD units/month, $p < 0.0001$; change in slope, 1.6064 ± 0.6534 OD units/month, $p = 0.0204$; Fig. 5B).

Concurrent Changes in RAGE, Aβ40, and Aβ42

The Aβ40 and Aβ42 were both measured in the same rats, permitting statistical assessment of the association of their relative changes across ages. Ordinary least squares regression indicated that there was a significant association between these changes of 0.3924 ± 0.0503 root (pg/mg) Aβ42 for each 1.0 root (pg/mg) change in Aβ40, $p < 0.0001$ adjusted $r^2 = 0.6736$. The amyloid concentrations were measured in different rats from those in which Western blot capillary RAGE or microvessel surface area RAGE expression was measured (which were also different samples), although all animals came from the same NIA rat colony and were genetically similar. The use of different animals precluded direct statistical analysis of their associations. Figure 6 allows for visual inspection of the similarities and differences of their changes in comparably aged animals.

Figure 6 double plots RAGE expression, as measured by immunostained surface area, and RAGE expression, as measured by Western blotting. These plots show a close association between the 2 RAGE measures. The Aβ40 and Aβ42 accumulation during aging in the rat is shown in parallel. When RAGE expression is level or possibly decreases during the first 9 months of life, amyloid is in the early part of its accelerating accumulation. Between 9 and 12 months, microvessel RAGE expression no longer degreases but begins to

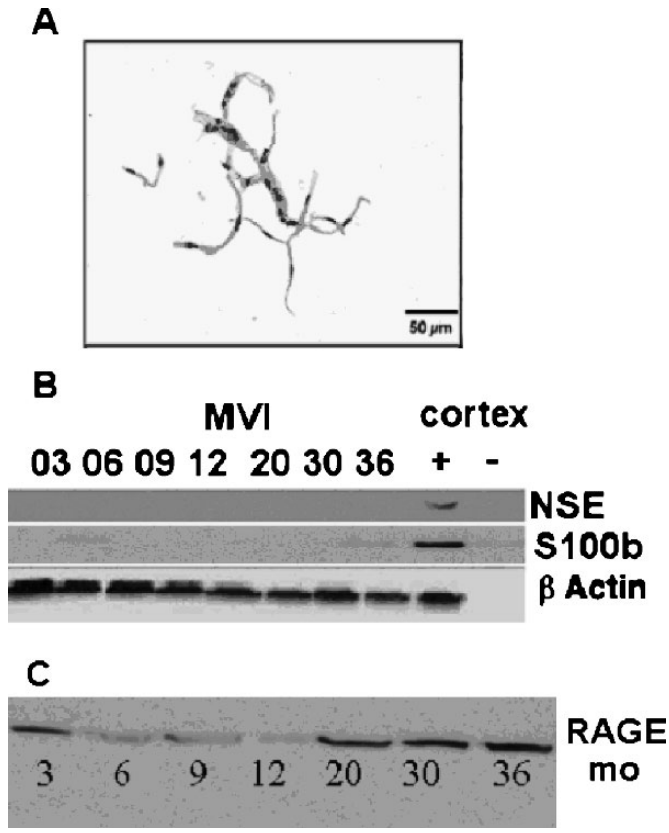

FIGURE 3. Microvessel isolations (MVIs). **(A)** Hematoxylin and eosin–stained whole mount of an MVI; it contains only microvessels. **(B)** Representative Western blot of a full series of age groups comparing neuron-specific enolase (NSE) and S100b expression in MVI to cortical homogenates. There is minimal staining for NSE and S100b across all age groups, confirming that neither neuronal membrane nor glial membrane proteins are detected in the protein extracted from the MVI preparations. Cortex = cortical homogenate (+, positive control; −, negative control; absence of specific antibody). **(C)** An example of Western blot receptor for advanced glycation end-products (RAGE) expression in MVI proteins extracted from all age groups. Note apparent decrease in RAGE immunoblots from 3 to 9 months and then a progressive increase from 12 to 36 months.

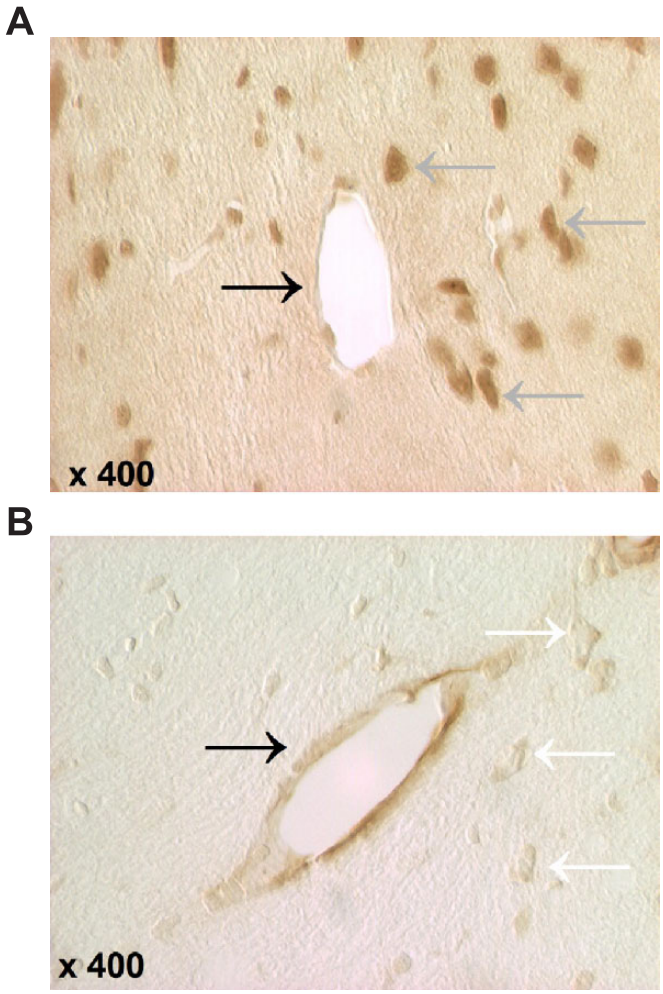

FIGURE 4. Immunostaining of hippocampal microvessel and neuronal receptor for advanced glycation end-products (RAGE) expression. **(A)** At 3 months, RAGE expression is primarily neuronal in its distribution (gray arrow); much less staining is seen in microvessels (black arrow). **(B)** At 30 months, microvessel RAGE immunoreactivity (black arrow) is increased, whereas neuronal staining (white arrow) is less evident.

increase in expression. Amyloid accumulates at its highest rate between 9 and 12 months. The RAGE continues to increase for the remainder of the life span of the rat, and Aβ42 continues to accumulate but at a slower rate. The Aβ40, as shown, does not accumulate significantly after 12 months.

DISCUSSION

Amyloid production, processing, and clearance are a very complex series of events that depend on a number of enzymatic and nonenzymatic carrier and transport steps. Once Aβ is released into the extracellular fluid space, however, its accumulation is primarily dependent on transport into and out of the CNS, mainly by way of the BBB in healthy young adults, and to a lesser extent by way of the cerebrospinal fluid circulation and via choroid plexus transport (10, 11, 13, 40, 41). Solute clearance is initiated by diffusion and the bulk flow of interstitial fluid to the perivascular, ventricular, and subarachnoid cerebrospinal fluid (13, 42, 43). In situ degradation accounts for a relatively small portion of Aβ disposal (44). Accumulation of Aβ, as demonstrated in this rat model, begins to occur surprisingly early in the aging process. There are also indications that changes in the brain associated with the age-related dementias begin in early middle age in humans. For example, studies of gene profiling in human brain aging have defined genes that are important to cognition with reduced expression soon after age 40 years (2, 3).

Studies of Aβ accumulation in Fischer rats have shown an increase in amyloid at several time points between 3 and 30 months by qualitative histological methods (45). Amyloid-β peptide has also been shown to be increased in cats aged 16 to 21 years compared with cats younger than 4 years (46) and in aged cognitively impaired rats (47). Amyloid has also been shown to accumulate in the senescence-accelerated-prone 8 mice, a mouse model of accelerated aging and AD (48). Systematic quantitative studies of Aβ deposition at multiple age points in rodent brains, however, are not easily found. Studies of amyloid deposition in human brains have shown that amyloid does accumulate in the brains of nondemented

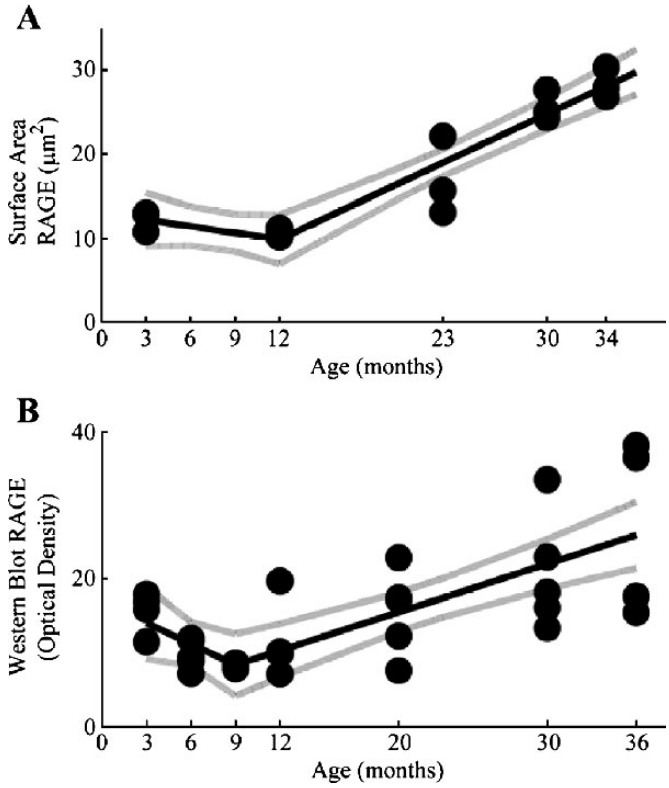

FIGURE 5. Piecewise regression of receptor for advanced glycation end-products (RAGE) expression as a function of age. **(A)** Immunohistochemistry surface area shows a nonsignificant decrease from 3 to 12 months followed by a substantial increase in RAGE expression up to 34 months ($p < 0.0001$). **(B)** Western blot RAGE expression shows a nonsignificant trend toward a decrease between 3 and 9 months ($p = 0.1072$) followed by a marked increase up to 36 months ($p < 0.0001$). Surface area RAGE expression, n = 3 rats per age group (8 fields per rat). Microvessel immunoblots, n = 3 to 5 per age group. Each *n* is 4 rat brains. Gray lines show 95% confidence interval.

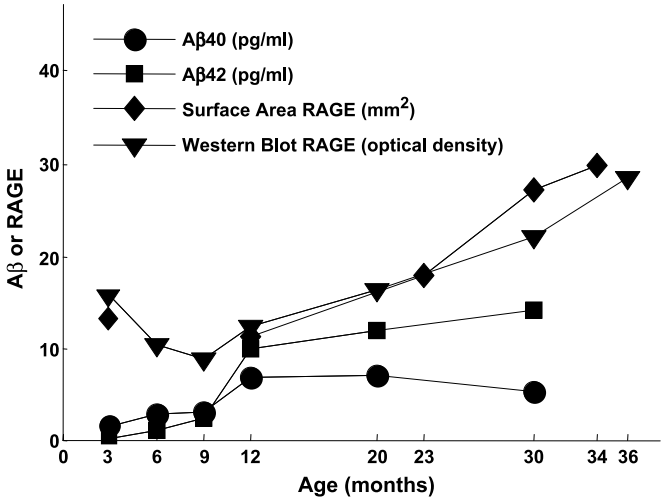

FIGURE 6. Relationship between the 2 measures of receptor for advanced glycation end-products (RAGE) expression and amyloid-β peptide (Aβ) accumulation. There is a close relationship between the means of the 2 different measures of RAGE expression. Between 9 and 12 months, there is an increase in both RAGE (Western blot) and mean Aβ levels. The expression of RAGE then increases throughout the lifetime of the rat (surface area and Western blot). The Aβ40 increases until 12 months and then plateaus, whereas Aβ42 continues to increase up to 30 months.

aging subjects, similar to what we found in the BN/F rat, but these studies are mainly histological and are primarily focused on elderly populations (49–55).

It is recognized that AD is a multifactorial disease, with aging playing a major role, and that Aβ accumulation seems to be an integral part of the disease (6); however, its accumulation in AD does not correlate well with the onset and progression of clinical impairment (50, 51). We show that Aβ accumulation in normal aging in the rat may also be multifactorial, including perhaps, different efflux transport rates of Aβ40 compared with Aβ42 and alterations in Aβ BBB transport receptor expression. In the young rat, Aβ40 is the more common of the amyloid peptides and seems to be transported out of the brain across the BBB with reasonable facility. By contrast, Aβ42 is less abundant early in life but also seems to be less easily transported out of the CNS. This is also true for measures of human Aβ transport in rats (56). In our study, Aβ42 began to accumulate at 9 months and rose rapidly between 9 and 12 months. At 3, 6, and 9 months, there is more Aβ40 than Aβ42, but by 12 months, the more difficult to transport Aβ42 predominates. After 12 months, Aβ40 concentration plateaus and seems to reach a new steady state wherein production and removal are seemingly in balance; however, Aβ42 continues to rise significantly up to age 30 months.

It is likely that the rise in Aβ42 is the result of more than a single factor. Our data demonstrate a parallel between Aβ42 accumulation and increasing capillary RAGE expression after 12 months; Aβ accumulation is likely less dependent on RAGE expression before 12 months. We have preliminary data suggesting that a decrease in efflux transporter expression (LRP-1 and P-gp) begins relatively early in aging (by ~9 months) and is progressively downregulated during the lifetime of the rat (57). These efflux transport alterations may play a part in both the early and later amyloid accumulation. We have also demonstrated a decrease in cerebrospinal fluid production and turnover later in aging that may play an important role in the later increase in amyloid burden (10, 57). The accumulation of Aβ with aging seems to be a combination of decreased efflux transport of endogenously generated Aβ and increasing influx transport from the vascular compartment. It is likely that the proportions from each Aβ source change with time.

We found IHC evidence for both neuronal and microvessel but not glial RAGE, and the immunoblots showed little or no evidence of RAGE-expressing cell populations other than microvessels in the MVIs. It has been reported that RAGE is only expressed on endothelial cell membranes and on certain cortical and hippocampal neurons in the brains of normal control patients and those with diabetes mellitus (22, 27). In AD patients, however, RAGE staining has been described in astrocytes, colocalizing with AGEs and Aβ (27). The MVIs showed positive bands for GFAP (data not shown), as has been described by others (58, 59). The GFAP bands are caused by the dense adherence of these protein fibrils to the capillary basement membrane.

The expression of RAGE is upregulated and downregulated in various cells at different ages. For example, RAGE expression in heart muscle is downregulated with age (25), and in an aging AD mouse model, microglial RAGE expression decreases as Aβ increases (60). The expression of RAGE is high in the brain during early development and then decreases with maturation (61). Between 9 and 12 months, when Aβ begins to rapidly accumulate in the cortex and hippocampus, we found that microvessel RAGE expression is the same or possibly less than at 3 months. By immunoblot measurements, RAGE seemed to decrease from 3 to 9 months and then began to increase up to 12 months. It seems unlikely, therefore, that microvessel RAGE expression has much influence on the initial increase in Aβ40 or Aβ42 retention, but the later Aβ42 accumulation may be caused, at least in part, by BBB RAGE overexpression. Certainly, the dramatic increase in capillary RAGE expression, from 12 months onward, parallels the marked rise in Aβ42 burden with aging. The parallels in RAGE overexpression in aging with those observed in early and late AD are also quite striking (20).

The expression of RAGE is dependent on environmental cues (28, 62), and its expression may have beneficial as well as detrimental biologic effects. During normal development, RAGE expression is high in the CNS and it interacts with amphoterin (high-mobility group box 1), a molecule that promotes neurite outgrowth (61). In diabetes, RAGE is overexpressed and binds AGEs, resulting in damage to multiple cell functions (28). The Aβ also interacts with RAGE, and endothelial RAGE expression increases dramatically in AD (19, 20). Ligands that interact with RAGE activate nuclear factor-κB, which signals a number of pathological events, including the upregulation of RAGE itself (28, 30, 32). Moreover, there is decreased methylation of the promoter region of the *RAGE* gene with aging that likely results in increased

RAGE expression (63). It seems likely that increased accumulation of AGEs and the increase in Aβ in early aging along with the increase in cytokines associated with both aging and AD lead to the decrease in promoter methylation and signal the upregulation of endothelial RAGE expression in the cerebral vasculature.

In summary, we have shown a relatively early increase in Aβ40 and an even earlier and progressive increase in Aβ42 accumulation with normal aging in the BN/F rat, beginning initially between 6 and 9 months and progressing rapidly between 9 and 12 months of age, that is, about one third of the way through the life span of the BN/F rat. We also show that RAGE expression, although initially trending toward a decrease after 3 months, begins to increase between age 9 and 12 months and progressively increases on brain capillary endothelium thereafter. This increase in capillary RAGE expression seems to be associated temporally, although not exclusively, with the later augmentation of the brain Aβ burden. Further studies are necessary to determine whether these same findings are present in aging human brains. If so, this increased age-related microvessel RAGE expression may be a significant part of the explanation as to why aging is the most important single risk factor for the development of AD.

ACKNOWLEDGMENTS

The authors thank Tracey Brooks and Dr Tom Davis (Department of Medical Pharmacology, University of Arizona College of Medicine, Tucson, AZ) for sharing the composition of the MVI buffer, and Stephanie Slone and Elizabeth Kenney (Department of Clinical Neuroscience, Aldrich Labs, Providence, RI) for the MVIs.

REFERENCES

1. National Institute of Aging. Alzheimer's Disease Unraveling the Mystery. US Department of Health and Human Services, 2002; NIH Publication Number 02–3782
2. Lu T, Pan Y, Kao SY, et al. Gene regulation and DNA damage in the aging human brain. Nature 2004;429:883–91
3. Yankner BA, Lu T, Loerch P. The aging brain. Annu Rev Pathol 2008;3:41–66
4. Hardy J. A hundred years of Alzheimer's disease research. Neuron 2006;52:3–13
5. Deane R, Zlokovic BV. Role of blood brain barrier in the pathogenesis of Alzheimer's disease. Curr Alzheimer Res 2007;4:191–97
6. Haass C, Selkoe DJ. Soluble protein oligomers in neurodegeneration: Lessons from the Alzheimer's amyloid β-peptide. Nat Rev Mol Cell Biol 2007;8:101–12
7. Rubenstein E. Relationship of senescence of cerebrospinal fluid circulatory system to dementias of the aged. Lancet 1998;351:283–85
8. Selkoe DJ. Toward a comprehensive theory for Alzheimer's disease. Hypothesis: Alzheimer's disease is caused by the cerebral accumulation and cytotoxicity of amyloid β-protein. Ann NY Acad Sci 2000;924:17–25
9. Trojanowski JQ, Lee V. Brain degeneration linked to "fatal attractions" of proteins in Alzheimer's disease and related disorders. J Alzheimers Dis 2001;3:117–19
10. Silverberg GD, Mayo M, Saul T, et al. Alzheimer's disease, normal-pressure hydrocephalus, and senescent changes in CSF circulatory physiology: A hypothesis. Lancet Neurol 2003;2:506–11
11. Zlokovic BV, Ghiso J, Mackic JB et al. Blood-brain barrier transport of circulating Alzheimer's amyloid β. Biochem Biophys Res Commun 1993;197:1034–40
12. Deane R, Wu Z, Zlokovic BV. RAGE (yin) versus LRP (yang) balance regulates Alzheimer amyloid β-peptide clearance through transport across the blood-brain barrier. Stroke 2004;35(suppl 1):2628–31
13. Shibata M, Yamada S, Kumar SR, et al. Clearance of Alzheimer's amyloid-β1-40 peptide from brain by LDL receptor–related protein-1 at the blood-brain barrier. J Clin Invest 2000;106:1489–99
14. Cirrito JR, Deane R, Fagan AM, et al. P-glycoprotein deficiency at the blood-brain barrier increases amyloid-β deposition in an Alzheimer disease mouse model. J Clin Invest 2005;115:3285–90
15. Deane R, Du Yan S, Submamaryan RK, et al. RAGE mediates amyloid b-peptide across the blood-brain barrier and accumulation in the brain. Nat Med 2003;9:907–13
16. Masters CL, Multhaup G, Simms G, et al. Neuronal origin of a cerebral amyloid: Neurofibrillary tangles of Alzheimer's disease contain the same protein as the amyloid of plaque cores and blood vessels. EMBO J 1985;4:2757–63
17. Siman R, Card JP, Nelson RB, et al. Expression of beta-amyloid precursor protein in reactive astrocytes following neuronal damage. Neuron 1989;3:275–85
18. Vitek MP, Battacharaya K, Glendening JM, et al. Advanced glycation end products contribute to amyloidosis in Alzheimer's disease. Proc Natl Acad Sci U S A 1994;91:4766–70
19. Donahue JE, Flaherty SL, Johanson CE, et al. RAGE, LRP-1, and amyloid-beta protein in Alzheimer's disease. Acta Neuropathol 2006;112:405–15
20. Miller MC, Taveres R, Johanson CE, et al. Hippocampal RAGE immunoreactivity in early and advanced Alzheimer's disease. Brain Res 2008;1230:273–80
21. Neeper M, Schmidt AM, Brett J, et al. Cloning and expression of a cell surface receptor for advanced glycosylation end products of proteins. J Biol Chem 1992;267:14998–5004
22. Brett J, Schmidt AM, Yan SD, et al. Survey of the distribution of a newly characterized receptor for advanced glycation end products in tissues. Am J Pathol 1993;143:1699–712
23. Ding O, Keller JN. Evaluation of rage isoforms, ligands and signaling in the brain. Biochim Biophys Acta 2005;1746:18–27
24. Schmidt AM, Stern DM. Receptor for age (RAGE) is a gene within the major histocompatibility class III region: Implications for host response mechanisms in homeostasis and chronic disease. Front Biosci 2001;6:D1151–60
25. Casselmann C, Reimann A, Friedrich I, et al. Age-dependent expression of advanced glycation end products receptor genes in the human heart. Gerontology 2004;50:127–34
26. Wautier JL, Schmidt AM. Protein glycation: A firm link to endothelial cell dysfunction. Circ Res 2004;95:233–38
27. Sasaki N, Toki S, Chowei H, et al. Immunohistochemical distribution of the receptor for advanced glycation end products in neurons and astrocytes in Alzheimer's disease. Brain Res 2001;888:256–62
28. Ramasamy R, Vannucci SJ, Du Yan SS, et al. Advanced glycation end products and RAGE: A common thread in aging, diabetes, neurodegeneration, and inflammation. Glycobiol 2005;15:16R–28R
29. Lin L. RAGE on the Toll road? Cell Mol Immunol 2006;3:351–58
30. Yan SD, Schmidt AM, Anderson GM, et al. Enhanced cellular oxidant stress by the interaction of advanced glycation end products with their receptors/binding proteins. J Biol Chem 1994;269:9889–97
31. Li J, Schmidt AM. Characterization and functional analysis of the promoter of RAGE, the receptor for advanced glycation end-products. J Biol Chem 1997;272:16498–506
32. Schmidt AM, Hasu M, Popov D, et al. Receptor for advanced glycation end products (AGEs) has a central role in vessel wall interactions and gene activation in response to circulating AGE proteins. Proc Natl Acad Sci U S A 1994;91:8807–11
33. Lohwasser C, Neureiter D, Weigle B, et al. The receptor for advanced glycation end products is highly expressed in the skin and upregulated by advanced glycation end products and tumor necrosis factor-alpha. J Invest Dermatol 2006;196:291–99
34. Banks WA, Robinson SM, Verma S, et al. Efflux of human and mouse amyloid beta proteins 1-40 and 1-42 from brain: Impairment in a mouse model of Alzheimer's disease. Neuroscience 2003;121:487–92
35. Wu LC, D'Amelio F, Fox RA, et al. Light microscopic image analysis system to quantify immunoreactive terminal area apposed to nerve cells. J Neurosci Methods 1997;74:89–96
36. Stopa EG, Butala P, Salloway S, et al. Cerebral cortical arteriolar angiopathy, vascular beta-amyloid, smooth muscle actin, Braak stage, and APOE genotype. Stroke 2008;39:814–21

37. Suzuki N, Cheung TT, Cai XD, et al. An increased percentage of long amyloid β protein secreted by familial amyloid β protein precursor (βAPP_{717}) mutants. Science 1994;264:336–40
38. Fukumoto H, Tomita T, Matsunaga H, et al. Primary cultures of neuronal and non-neuronal rat brain cells secrete similar proportions of amyloid β peptides ending at Aβ40 and Aβ42. Neuroreport 1999;10:2965–69
39. Yousif S, Marie-Claire C, Roux F, et al. Expression of drug transporters at the blood-brain barrier using an optimized isolated rat brain microvessel strategy. Brain Res 2007;1134:1–11
40. Silverberg GD, Heit G, Huhn S, et al. The cerebrospinal fluid production rate is reduced in dementia of the Alzheimer's type. Neurology 2001;57:1763–66
41. Deane R, Sagare A, Hamm K, et al. ApoE isoform–specific disruption of amyloid β peptide clearance from mouse brain. J Clin Invest 2008;118:4002–13
42. Davson H, Oldendorf WH. Symposium on membrane transport. Transport in the central nervous system. Proc R Soc Med 1967;60:326–29
43. Weller RO. Pathology of cerebrospinal fluid and interstitial fluid of the CNS: Significance for Alzheimer's disease, prion disorders and multiple sclerosis. J Neuropathol Exp Neurol 1998;57:885–94
44. Iwata N, Tsubuki S, Takaki Y, et al. Identification of the major Abeta1-42–degrading catabolic pathway in brain parenchyma: Suppression leads to biochemical and pathological deposition. Nat Med 2000;6:143–50
45. Preston JE. Aging choroid plexus–cerebrospinal system. Microsc Res Tech 2001;52:31–37
46. Head E, Moffat K, Das P, et al. Beta-amyloid deposition and tau phosphorylation in clinically characterized aged cats. Neurobiol Aging 2005;26:749–63
47. Vaucher E, Aumont N, Pearson D, et al. Amyloid beta peptide levels and its effect on hippocampal acetylcholine release in aged, cognitively-impaired and -unimpaired rats. J Chem Neuroanat 2001;21:323–29
48. Banks WA, Farr SA, Morley JE, et al. Anti-amyloid beta protein antibody passage across the blood-brain barrier in the SAMP8 mouse model of Alzheimer's disease: An age-related selective uptake with reversal of learning impairment. Exp Neurol 2007;206:248–56
49. Katzman R, Terry R, DeTeresa R, et al. Clinical, pathological, and neurochemical changes in dementia. Ann Neurol 1988;23:138–44
50. Braak H, Braak E. Neuropathological staging of Alzheimer-related changes. Acta Neuropathol 1991;82:239–59
51. Braak H, Braak E. Demonstration of amyloid deposits and neurofibrillary changes in whole brain sections. Brain Pathol 1991;1:213–16
52. Price J, Davis P, Morris J, White D. The distribution of tangles, plaques, and related immunohistochemical markers in healthy aging and Alzheimer's disease. Neurobiol Aging 1991;12:295–312
53. Arriagada P, Marzloff K, Hyman B. Distribution of Alzheimer-type pathologic changes in nondemented elderly individuals matches the pattern in Alzheimer's disease. Neurology 1992;42:1681–88
54. Giannakopoulos P, Hof P, Giannakopoulos AS, Herrmann F, Michel JP, Bouras C. Regional distribution of neurofibrillary tangles and senile plaques in the cerebral cortex of very old patients. Arch Neurol 1995;52:1150–60
55. Davis D, Schmitt F, Wekstein D, Markesbery W. Alzheimer neuropathologic alterations in aged cognitively normal subjects. J Neuropathol Exp Neurol 1999;58:376–88
56. Bell RD, Sagare AP, Friedman AE, et al. Transport pathways for clearance of human Alzheimer's amyloid beta-peptide and apolipoproteins E and J in the mouse central nervous system. J Cereb Blood Flow Metab 2006;27:909–18
57. Silverberg GD, Caralopoulos IN, Slone SL, et al. Amyloid and Tau accumulation precede CSF production decline in normal aging [Abstract]. CSF Res 2009;6(suppl 1):S38.
58. White FP, Dutton GR, Norenberg MD. Microvessels isolated from rat brain: Localization of astrocyte processes by immunohistochemical techniques. J Neurochem 1981;36:328–32
59. Moro V, Kacem K, Springhetti V, et al. Microvessels isolated from brain: Localization of muscarinic sites by radioligand binding and immunofluorescent techniques. J Cereb Blood Flow Metab 1995;15:1082–92
60. Hickman SE, Allison EK, El Koury J. Microglial dysfunction and defective beta-amyloid clearance pathways in aging Alzheimer's disease mice. J Neurosci 2008;28:8354–60
61. Leclerc E, Fritz G, Weibel M, et al. S100B and S100A6 differentially modulate cell survival by interacting with distinct RAGE (receptor for advanced glycation end products) immunoglobulin domains. J Biol Chem 2007;282:31317–31
62. Schmidt AM, Wautier J-L, Stern D, et al. RAGE: A receptor with a taste for multiple ligands and varied pathophysiologic states. In: O'Malley BW, ed. *Hormones and Signaling*. Amsterdam, Holland: Elsevier Inc, 1998;41–63
63. Tohgi H, Utsugisawa K, Nagane Y, et al. Decrease with age in methylcytosines in the promoter region of receptor for advanced glycation end products (RAGE) gene in autopsy human cortex. Brain Res Mol Brain Res 1999;65:124–28

APPENDIX

Western and Dot Blotting for Aβ40 and Aβ42

Quantitative ELISA measurements for Aβ40 and Aβ42 are highly sensitive and selective, but cross-reactivity of the C-terminal antibodies used in the ELISA determinations with other proteins cannot be completely excluded (Suzuki N, Cheung TT, Cai XD, et al. An increased percentage of long amyloid β protein secreted by familial amyloid β protein precursor (βAPP_{717}) mutants. *Science*. 1994;264:336–340; Fukumoto H, Tomita T, Matsunaga H, et al. Primary cultures of neuronal and non-neuronal rat brain cells secrete similar proportions of amyloid β peptides ending at Aβ40 and Aβ42. *Neuroreport*. 1999;10:2965–2969). To ensure that the age-related increases in Aβ40 and Aβ42 demonstrated by ELISA and qualitatively by IHC were correct, we sought to verify absolute increases in Aβ40 and Aβ42 with aging by Western blotting and dot blotting.

Western blotting for Aβ40 and Aβ42 (n = 5 for each age group) was performed according to Ida et al (Ida N, Hartmann T, Pantel J, et al. Analysis of heterogeneous beta A4 peptides in human cerebrospinal fluid and blood by a newly developed sensitive Western blot assay. *J Biol Chem*. 1996;271:22908–22914) with minor modifications. The samples containing the brain homogenates in sample buffer (Invitrogen, NuPAGE SDS Sample Buffer 4×) containing 8M urea (BioRad, Hercules, CA) were mixed with 2 μL of reducing agent (Invitrogen, NuPAGE Sample reducing agent 10×), vortexed, heated at 70°C for 10 minutes, and centrifuged at 11,900 × *g* for 5 minutes. Separation was done with 4% to 12% sodium dodecyl sulfate–polyacrylamide gel electrophoresis (Invitrogen, 4%–12% NuPAGE Bis-Tris-Gel) with 2-(N-morpholino) ethanesulfonic acid running buffer (Invitrogen, NuPAGE MES SDS Running Buffer). Separated proteins on the gels were electrophoretically transferred via transfer buffer (Invitrogen, NuPAGE Transfer Buffer 20×) + 10%MeOH (Fisher Scientific, Pittsburgh, PA). Blots were transferred onto 0.2-μm nitrocellulose membrane (Amersham Bioscience, Sunnyvale, CA) at 25V for 1 hour. The blotted membrane was heated for 3 minutes with microwaves (900 W) in boiling TBS to enhance the binding; nonspecific binding sites were blocked with 5% skim milk in TBST for at least 30 minutes. After rinsing twice and washing the membrane with fresh TBST (5 minutes), the Aβ antibodies 1–40 and 1–42 (Abcam) diluted in TBST were added and incubated overnight at 4°C. The membrane was first washed with TBST and then soaked (3 × 10 minutes) in fresh TBST, and the bound antibody detected by horseradish peroxidase–linked secondary antibody (Vector) diluted 1:50,000 in

TBST. The same washing and soaking cycle with TBST was applied to the membrane. Visualization was performed using the enhanced chemiluminescence detection system (Pierce) according to the manufacturer's instruction by exposing the membrane to an autoradiography film (Fisher). Protein was determined by the bicinchoninic method; 40 μg was loaded per well, and bands were compared with β-actin (Sigma) loading controls. Positive and negative controls were also performed (data not shown). Positive Aβ controls were Aβ40 and Aβ42 standards (rodent-specific Aβ40, Catalog No. H-5638, and Aβ42, Catalog No. H-5966; Bachem, Torrance, CA). Negative controls were the absence of the primary antibody. Differences in Aβ40 and Aβ42 concentrations between 3 and 30 months of age were determined by OD measurements using a calibrated OD step tablet that converts pixel density to OD values (ImageJ program, http://rsb.info.nih.gov/ij/download.hyml).

We also performed dot blots for the 2 peptides at 3 and 30 months (n = 4 for each age group); 2-μL samples of lysate were added to a nitrocellulose membrane (Amersham Bioscience) and dried. The membrane was treated with either Aβ40 or Aβ42 antibody and exposed to autoradiography. The ImageJ program was used to determine the integrated area of pixel density of the Aβ40 and Aβ42 dot blots. The integrated density was measured by outlining each dot after background correction. Positive and negative controls were also tested (data not shown). Student *t*-test was used to compare Western blot OD values and dot blot integrated densities at 3 and 30 months for the peptides.

As others have reported, we found that measurements of Aβ40 and Aβ42 by Western blotting are technically difficult in the nontransgenic rat (Lanz TA, Schachter JB. Demonstration of a common artifact in immunosorbent assays of brain extracts: development of a solid-phase extraction protocol to enable measurement of amyloid-β from wild-type rodent brains. *J Neurosci Methods*. 2006;157:71–81). The 2 peptides oligomerize rapidly in wild-type rats so that monomeric Aβ40 and Aβ42 are scant and not representative of the amount of Aβ peptides present. In the technique that we used, the most abundant form of Aβ40 and Aβ42 was the trimeric oligomer that migrates at 14 kd; therefore, the trimeric bands were selected for comparisons.

There was a marked increase in Aβ40 and Aβ42 concentrations between 3 and 30 months in both the Western blots and dot blots. For Aβ40, the OD value for the Western blot trimeric form at 3 months was 0.12 ± 0.02 (mean ± SEM); at 30 months, it was 0.58 ± 0.02, $p = 0.0001$ (Figure, Supplemental Digital Content 1, http://links.lww.com/NEN/A71). The integrated density value for the dot blot was also increased at 30 months compared with 3 months. For Aβ40, the integrated area of pixel density at 3 months was 3284 ± 839 and 6031 ± 840 at 30 months, $p = 0.03$. For Aβ42, the Western blot trimeric oligomer OD value at 3 months was 0.10 ± 0.01; at 30 months, it was 0.31 ± 0.04, $p < 0.002$ (Figure, Supplemental Figure 2, http://links.lww.com/NEN/A72). The integrated area of pixel density for the dot blot was also increased in the aged animals compared with the young. For Aβ42, the integrated area of pixel density at 3 months was 2,244 ± 203; at 30 months, it was 4,084 ± 312, $p = 0.002$.

These data show an absolute increase in Aβ40 and Aβ42 in rats at 3 versus 30 months of age. The few articles referencing measurement of Aβ40 and Aβ42 in wild-type rats by Western blotting also show that oligomeric forms predominate; most commonly, they are the trimeric form and larger oligomers (Han F, Ali Raie A, Shioda N, et al. Accumulation of beta-amyloid in the brain microvessels accompanies increased hyperphosphorylated Tau proteins following microsphere embolism in aged rats. *Neuroscience*. 2008;153:414–427; Bennett SA, Pappas BA, Stevens WD, et al. Cleavage of amyloid precursor protein elicited by chronic cerebral hypofusion. *Neurobiol Aging*. 2000;21:207–214). Our data are similar to these reported measurements and support our ELISA measurements, although the latter are more sensitive and quantitative.